INSTITUTUL
DE
MATEMATICA

INSTITUTUL NATIONAL
PENTRU CREATIE
STIINTIFICA SI TEHNICA

ISSN 0250-3638

SIMULATION OF HOT EXTRUSION BY USING HOT TORSION TECHNIQUES

by

E.SOÓS, C.TEODOSIU, V.NICOLAE, C.G.RADU

PREPRINT SERIES IN MATHEMATICS
No.40/1980

BUCURESTI

SIMULATION OF HOT EXTRUSION BY USING HOT TORSION TECHNIQUES

by

E.SOÓS*), C.TEODOSIU**), V.NICOLAE**), C.G.RADU***)

August 1980

*) Department of Mathematics, National Institute for Scientific and Technical Creation, Bd.Pacii 220, 79622 Bucharest, Romania.

**) Institute for Physics and Technology of Materials, Department of Solid Mechanics, 70701 Bucharest, Romania.

***) Institute for Metallurgical Research, 77769 Bucharest, Romania.

SIMULATION OF HOT EXTRUSION BY USING HOT TORSION TECHNIQUES

by E.SOÓS, C.TEODOSIU, V.NICOLAE, C.G.RADU

Abstract

The simulation of hot working processes by hot torsion techniques provides an inexpensive and convenient method for testing and optimizing new forming technologies. The present paper concerns the simulation of hot extrusion with application to the extrusion of the AISI 316L austenitic stainless steel.

SIMULATION OF HOT EXTRUSION BY USING HOT TORSION TECHNIQUES.

by E.SOOS[x], C.TEODOSIU[xx], V.NICOLAE[xx], C.G.RADU[xxx]

The most reliable method of determining hot workability is to process materials under plant conditions, where the variables inherent in the material (composition, size, shape, microstructure) and the variables inherent in the process (strain rate and stress fields, lubrication, temperature) are simultaneously covered. However, this method is expensive and the obvious advantages of laboratory tests, e.g. ease of checking different casts, ease of determining optimum conditions for new materials, close control of variables, and possibility of relating structure and properties have led to the development of a number of such tests.

Hot torsion tests provide a rather simple means for the laboratory investigation of the hot workability of metals and alloys, as high strains characteristic for extrusion can be attained at constant surface strain rate and quantitative estimates

---

x) National Institute for Scientific and Technical Creation, 79622 Bucharest.

xx) Institute for Physics and Technology of Materials, Department of Solid Mechanics, 7o7o1 Bucharest, Romania

xxx) Institute for Metallurgical Research, 77769 Bucharest

of both flow stress and ductility can be obtained. Also, programmed deformation to simulate rolling or forging schedules can be applied relatively simple.

1. SIMULATION CRITERIA

As simulation is not a reproduction, but a modelling of real processes, it is necessary to adopt some criteria of equivalence between laboratory and industrial conditions in order to obtain a correct evaluation of the hot workability and of the structural parameters. Two such criteria have been proposed by the present authors [1, 2], namely the equality of the final strain intensities and of the plastic work done per unit volume during the deformation in the technological process and the torsion test.

According to the theory of plastic flow of rigid-viscoplastic materials we adopt for the plastic deformation the three-dimensional constitutive equation

$$S_{ij} = \frac{2}{3}\frac{\sigma}{\dot{\varepsilon}} D_{ij} \quad , \quad i,j = 1,2,3, \qquad (1.1.)$$

where S_{ij} and D_{ij} are the Cartesian components of the deviator of the stress tensor and of the (isochoric) plastic strain rate tensor, respectively, whereas σ and $\dot{\varepsilon}$ are the stress and strain rate intensities, which are given by

$$\sigma = \sqrt{\frac{3}{2}\sum_{i,j=1}^{3} S_{ij} S_{ij}} \quad , \quad \dot{\varepsilon} = \sqrt{\frac{2}{3}\sum_{i,j=1}^{3} D_{ij} D_{ij}} \, . \qquad (1.2)$$

Taking into account that $\underset{\sim}{S}$ is a deviator, and the plastic deformation proceeds without change of volume, we have

$$S_{11} + S_{22} + S_{33} = 0 \, , \qquad D_{11} + D_{22} + D_{33} = 0, \qquad (1.3)$$

and (1.2) can be written after some manipulation under the form

$$\sigma = \frac{1}{\sqrt{2}} \sqrt{(S_{11}-S_{22})^2+(S_{22}-S_{33})^2+(S_{33}-S_{11})^2+6(S_{12}^2+S_{23}^2+S_{13}^2)}, \quad (1.4)$$

$$\dot{\varepsilon} = \frac{\sqrt{2}}{3} \sqrt{(D_{11}-D_{22})^2+(D_{22}-D_{33})^2+(D_{33}-D_{11})^2+6(D_{12}^2+D_{23}^2+D_{13}^2)}. \quad (1.5)$$

By using the physical components of the tensors $\underset{\sim}{S}$ and $\underset{\sim}{D}$ in the spherical co-ordinates $(r, \theta, \varphi,)$, Eqs. (1.3) - (1.5) become

$$S_{rr} + S_{\theta\theta} + S_{\varphi\varphi} = 0, \qquad D_{rr} + D_{\theta\theta} + D_{\varphi\varphi} = 0, \quad (1.6)$$

$$\sigma = \frac{1}{\sqrt{2}} \sqrt{(S_{rr}-S_{\theta\theta})^2+(S_{\theta\theta}-S_{\varphi\varphi})^2+(S_{\varphi\varphi}-S_{rr})^2+6(S_{r\theta}^2+S_{\theta\varphi}^2+S_{r\varphi}^2)}, \quad (1.7)$$

$$\dot{\varepsilon} = \frac{\sqrt{2}}{3} \sqrt{(D_{rr}-D_{\theta\theta})^2+(D_{\theta\theta}-D_{\varphi\varphi})^2+(D_{\varphi\varphi}-D_{rr})^2+6(D_{r\theta}^2+D_{\theta\varphi}^2+D_{r\varphi}^2)}. \quad (1.8)$$

The plastic work done per unit time and unit volume is given by the relation

$$w = \sum_{i,j=1}^{3} S_{ij} D_{ij} = \sigma \dot{\varepsilon}. \quad (1.9)$$

Consequently, the plastic work done per unit volume up to a current time t is

$$L(t) = \int_0^t w\, dt = \int_0^t \sigma \dot{\varepsilon}\, dt = \int_0^{\varepsilon} \sigma\, d\varepsilon, \quad (1.10)$$

where

$$\varepsilon = \int_0^t \dot{\varepsilon}\, dt \quad (1.11)$$

is the strain intensity at time t.

In order to establish a correspondence between the torsion test (T) and an industrial hot working process (P) we adopt [1] the following criteria of equivalence

$$\varepsilon_f^P = \varepsilon_{sf}^T, \quad (1.12)$$

$$L_f^P = L_{sf}^T, \quad (1.13)$$

where ε_f^P is the final value of the hot working strain intensity, ε_{sf}^T is the final value of the torsion surface strain intensity,

L_f^P is the final plastic work done per unit volume in the hot working process, and L_{sf}^T is final surface value of the plastic work done per unit volume in torsion. By (1.1o) and (1.12), Eq. (1.13) also implies that

$$\int_0^{\varepsilon_f^P} \sigma^P \, d\varepsilon^P = \int_0^{\varepsilon_{sf}^T} \sigma_s^T \, d\varepsilon_s^T , \qquad (1.14)$$

where σ^P is the stress intensity in the hot working process, and σ_s^T is surface stress intensity in the torsion test. The equivalence criteria (1.12) and (1.14) assure the reproduction of the main features of the hot workability of the material, namely ductility and deformation strength. As shown by complementary metallurgical evidence [3], the above criteria provide a better simulation of hot working processes than the usual simulation that is based on condition (1.12) and on the reproduction of the temperature schedule irrespective of the torsion speed [4 - 11].

It should be mentioned that industrial hot working processes are characterized by inhomogeneous strain rate, stress, and thermal fields. Therefore, the equivalence criteria must be applied for each characteristic point of the deformed material.

In the following we shall apply the simulation procedure to the hot extrusion of an AISI 316 L stainless steel.

2. CONSTITUTIVE EQUATIONS

Torsion tests conducted on a SETARAM machine in the range 9oo - 12oo°C at surface strain rate intensities between o.oo7 and 5.441 s^{-1} on an AISI 316 L stainless steel have been used [12] to determine the explicit dependence $\sigma = \sigma(\varepsilon, \dot{\varepsilon}, T)$. In the range of hot deformation this equation can be written as

$$\sigma = \sigma(\varepsilon, Z), \tag{2.1}$$

where

$$Z = \dot{\varepsilon} \exp \frac{Q}{RT} \tag{2.2}$$

is the Zener-Hollomon parameter, T is the absolute temperature, Q is the activation energy of the softening process (recovery or recrystallization), and R = 8.314 J/K mol is the gas constant.

The surface value σ_s^T of σ^T has been calculated by using the relation [13]

$$\sigma_s^T = \frac{\sqrt{3}}{2\pi r_0^3}\left(3\Gamma + \varepsilon_s^T \frac{\partial \Gamma}{\partial \varepsilon_s^T} + \dot{\varepsilon}_s^T \frac{\partial \Gamma}{\partial \dot{\varepsilon}_s^T}\right), \tag{2.3}$$

where Γ is the torque. For the AISI 316L the terms containing the derivatives of Γ with respect to ε_s^T and $\dot{\varepsilon}_s^T$ can be neglected, and hence Eq. (2.3) reduces to the simplified formula

$$\sigma_s^T = \frac{3\Gamma\sqrt{3}}{2\pi r_0^3}, \tag{2.4}$$

or

$$\sigma(\varepsilon_s^T, Z_s^T) = \frac{3\sqrt{3}}{2\pi r_0^3}\,\Gamma(\varepsilon_s^T, Z_s^T), \tag{2.5}$$

where

$$Z_s^T = \dot{\varepsilon}_s^T \exp \frac{Q}{RT_i^T}. \tag{2.6}$$

Moreover, since Z_s^T can be varied independently of ε_s^T, Eq.(2.5) still holds for arbitrary values of ε and Z. This remark allows the straightforward derivation of the equation (2.1) by using the correlation $\Gamma = \Gamma(\varepsilon_s^T, Z_s^T)$ obtained from torsion tests. To the onset of dynamic recrystallization the final result [12] reads

$$\sigma = \begin{cases} [a + c(1 - e^{-n\varepsilon})] \ln(Z/b) & \text{for } Z \leq Z_\ell \\ \sigma_\ell^* + c(1 - e^{-n\varepsilon}) \ln(Z/b) & \text{for } Z > Z_\ell, \end{cases} \tag{2.7}$$

where

$$Q = 499 \text{ kJ/mol}, \quad n = 3.86, \quad b = e^{36.23}\ s^{-1}$$
$$a = 1o.o7 \text{ MPa}, \quad c = 11.13 \text{ MPa}, \tag{2.8}$$

whereas

$$Z_\ell = e^{48.o8}\ s^{-1}, \quad \sigma_\ell^* = 121.24 \text{ MPa} \tag{2.9}$$

are certain critical values of Z and of the effective flow stress intensity σ^*, respectively, defining the transition from the thermal to the athermal flow regime.

The surface value of the plastic work done per unit volume up to a current time t during the torsion test is

$$L_s^T = \int_0^{\varepsilon_s^T} \sigma_s^T \, d\varepsilon_s^T . \tag{2.1o}$$

By (2.4) this relation becomes

$$L_s^T = \frac{3\sqrt{3}}{2\pi r_o^3} \int_0^{\varepsilon_s^T} \Gamma \, d\varepsilon_s^T , \tag{2.11}$$

where the integral in the right-hand side can be calculated numerically from experimental data. Furthermore, Eq. (2.11) can be replaced with a very good approximation by

$$L_s^T = k_L \varepsilon_s^T , \tag{2.12}$$

where k_L is a coefficient depending on T_i^T and $\dot{\varepsilon}_s^T$. The best fit of experimental results gives

$$k_L = a_L \left(\ln \dot{\varepsilon}_s^T + \frac{Q_L}{R T_i^T} - \ln b_L \right), \tag{2.13}$$

where

$$Q_L = 61o \text{ kJ/mol}, \quad a_L = 14.49 \text{ MPa}, \quad b_L = e^{43.89}\ s^{-1}. \tag{2.14}$$

Eqs. (2.12) and (2.13) will be used in the following, in conjunction with the equivalence criteria (1.12) and (1.13), for determining the initial temperature T_i^T of the torsion test.

3. SIMPLIFYING HYPOTHESES

The application of the equivalence criteria obviously requires the knowledge of the evolution of termokinematic fields during the hot working process and the torsion test, and this implies the solving of very complicated non-linear boundary-value problems. To avoid this formidable task we adopt the following simplifying hypotheses:

(i) The physical components of the strain rate tensor $\underset{\sim}{D}$ in the spherical co-ordinates (r, φ, θ) are calculated by the relations

$$\left.\begin{aligned} D_{rr} &= \frac{\partial v_r}{\partial r}, \qquad D_{r\theta} = \frac{1}{2}\left(\frac{\partial v_\theta}{\partial r} + \frac{1}{r}\frac{\partial v_r}{\partial \theta} - \frac{v_\theta}{r}\right), \\ D_{r\varphi} &= \frac{1}{2}\left(\frac{1}{r\sin\theta}\frac{\partial v_r}{\partial \varphi} + \frac{\partial v_\varphi}{\partial r} - \frac{v_\varphi}{r}\right), \quad D_{\theta\theta} = \frac{1}{r}\frac{\partial v_\theta}{\partial \theta} + \frac{v_r}{r}, \\ D_{\theta\varphi} &= \frac{1}{2}\left(\frac{1}{r\sin\theta}\frac{\partial v_\theta}{\partial \varphi} + \frac{1}{r}\frac{\partial v_\varphi}{\partial \theta} - \frac{v_\varphi}{r}\operatorname{ctg}\theta\right), \\ D_{\varphi\varphi} &= \frac{1}{r\sin\theta}\frac{\partial v_\varphi}{\partial \varphi} + \frac{v_r}{r} + \frac{v_\theta}{r}\operatorname{ctg}\theta, \end{aligned}\right\} \tag{3.1}$$

from an admissible velocity field $\underset{\sim}{v}\,(v_r, v_\varphi, v_\theta)$ that satisfies the kinematic boundary conditions and the incompressibility condition $(1.6)_2$.

(ii) The working process is assumed to proceed adiabatically, the entire amount of heat resulted from the plastic deformation of each element being consumed for the increase of its temperature. Thus, the temperature at time t is given by

$$T^P(t) = T_i^P + \frac{1}{\rho c_v} L^P(t), \tag{3.2}$$

where T_i^P is the initial temperature of the volume element at the beginning of the deformation, ρ is the mass density, and c_v is the specific heat at constant volume.

(iii) The contribution of the friction work to the thermal balance is neglected.

The validity of the above assumptions can be partly tested by measuring the variation of the stress intensity during the torsion test and comparing it with the corresponding values given by Eq.(2.7), where ε and Z are calculated by using (i) and (ii) for the simulated working process. It should be mentioned, however, that the final verification of the simulation procedure has to be obtained by comparing the microstructures of the sample and of the worked material, as well as by measuring the force parameters in the working process and comparing them with those calculated from laboratory results.

The above simulation procedure will be illustrated in the next section for the case of hot extrusion of the AISI 316L austenitic stainless steel. Further examples of the simulation technique for hot strip rolling and forging are given elsewhere [2, 14] .

4. ADMISSIBLE KINEMATIC FIELD FOR EXTRUSION

As mentioned in the previous section, the simulation of the extrusion of cylindrical bars is based on the selection of a kinematically admissible velocity field [15] . The billet is divided into four zones in which the velocity field is assumed as being continuous. The zones are separated by the spherical surfaces Σ_i and Σ_f with centre at O and radius r_i and r_f, respectively, and by the conical surface with apex at O (Fig.1).

It is assumed that the material in zones I and III behaves like a rigid ; the only non-zero component of the velocity is v_z and its constant values are denoted by v_i and v_f, respectively.

By virtue of the incompressibility condition, and using the notations in Fig.1 , we have

$$v_i = v_f \left(\frac{R_f}{R_i}\right)^2 . \tag{4.1}$$

In zone II the velocity is directed toward the apex O of the cone and the velocity field has cylindrical symmetry. Denoting by v the magnitude of the velocity, using the spherical co-ordinates (r, φ, θ) , and taking again into account the incompressibility condition, we have

$$v_r = -v = -v\, r_f^2 \frac{\cos\theta}{r^2} , \quad v_\theta = v_\varphi = 0 . \tag{4.2}$$

In zone IV, called the dead zone, the material is at rest ; the existence of this region depends on the die geometry, as well as on the friction between the billet and the die.

Across the surfaces Σ_i and Σ_f the normal component of the velocity is continuous, while its tangential component has the jumps

$$\Delta v_i = v_i \sin\theta \ \text{ on } \Sigma_i , \qquad \Delta v_f = v_f \sin\theta \ \text{ on } \Sigma_f . \tag{4.3}$$

By introducing (4.2) into (3.1) we infer that the non-zero components of the strain rate tensor $\underset{\sim}{D}$ are given by

$$D_{rr} = -2 D_{\varphi\varphi} = -2 D_{\theta\theta} = 2 v_f r_f^2 \frac{\cos\theta}{r^3} ,$$
$$D_{r\theta} = \frac{1}{2} v_f r_f^2 \frac{\sin\theta}{r^2} . \tag{4.4}$$

Substituting this result into (1.8) gives

$$\dot{\varepsilon}^E = 2 v_f r_f^2 \frac{1}{r^3} \sqrt{1 - \frac{11}{12}\sin^2\theta} . \tag{4.5}$$

Next, from (4.5) and (1.11) and taking into account that

$$dt = -\frac{dr}{v} = -\frac{r^2 dr}{v_f r_f^2 \cos\theta},$$

we deduce that the strain intensity is given by

$$\varepsilon^E = \frac{2\sqrt{1-\frac{11}{12}\sin^2\theta}}{\cos\theta} \ln\frac{r_i}{r} \tag{4.6}$$

and has the final value

$$\varepsilon_f^E = \frac{2\sqrt{1-\frac{11}{12}\sin^2\theta}}{\cos\theta} \ln\frac{R_i}{R_f}. \tag{4.7}$$

By eliminating r between Eqs. (4.6) and (4.5) we may express $\dot{\varepsilon}$ as a function of ε for $\theta =$ const. through the relation

$$\dot{\varepsilon}^E = \frac{2v_i}{r_i}\sqrt{1-\frac{11}{12}\sin^2\theta}\ \exp\frac{3\varepsilon^E\cos\theta}{2\sqrt{1-\frac{11}{12}\sin^2\theta}}. \tag{4.8}$$

In order to calculate the jump in strain across the surface Σ_i we assume that v_φ decreases linearly in a small elapse of time t_1 from $v_i \sin\varphi$ to 0, i.e.

$$v_\varphi = v_i(1-t/t_1)\sin\varphi, \qquad t\in[0,t_1]. \tag{4.9}$$

Introducing (4.9) into $(3.1)_2$, and considering that for $t \in [0, t_1]$ we can take $r \simeq r_i$ and hence $v_r = -v_i\cos\varphi$, we obtain

$$D_{r\theta} = \frac{1}{2}\frac{tg\theta}{t_1}\left(1+\frac{v_i t\cos\theta}{r_i - v_i t\cos\theta}\right) \approx \frac{1}{2}\frac{tg\theta}{t_1}. \tag{4.10}$$

Neglecting the other components of $\underset{\sim}{D}$ with respect to $D_{r\theta}$ we obtain from (4.10), (1.8), and (1.11) the jump $\Delta\varepsilon_i$ in the strain intensity across the surface Σ_i:

$$\Delta\varepsilon_i = \int_0^{t_1}\dot{\varepsilon}^E dt = \frac{2}{\sqrt{3}}\int_0^{t_1} D_{r\theta}\,dt = \frac{1}{\sqrt{3}}tg\theta. \tag{4.11}$$

This result shows that the jump in the strain intensity does not depend on r and t, and hence the jump $\Delta\varepsilon_f$ across the surface Σ_f is equally given by (4.11).

5. PLASTIC WORK DISSIPATED DURING EXTRUSION

Denoting by L^E the work done per unit volume up to a current strain intensity ε^E in the zone between the surfaces Σ_i and Σ_f we have from (1.1o):

$$L^E = \int_0^{\varepsilon^E} \sigma(\varepsilon, Z^E)\, d\varepsilon, \tag{5.1}$$

where ε^E is given by (4.6) and σ by (2.7).

The contribution ΔL_i to the total work of the rapid variation of $D_{r\theta}$ during the time elapse t_1 in the neighbourhood of Σ_i can be evaluated by the formula

$$\Delta L_i = \int_0^{t_1} \sigma(\varepsilon^E, Z^E)\, \dot{\varepsilon}^E\, dt = \frac{1}{\sqrt{3}}\, \sigma_\ell^*\, tg\theta. \tag{5.2}$$

In deriving the last relation we have taken into account that t_1, is very small, which implies that ε^E is very small, whereas $\dot{\varepsilon}^E$ and Z^E are very large during this time. Consequently, considering also $(2.7)_2$, the function $\sigma(\varepsilon^E, Z^E)$ has been replaced in (4.13) by the constant value σ_ℓ^*.

A similar reasoning gives for the work ΔL_f corresponding to $D_{r\theta}$ at traversing the surface Σ_f

$$\Delta L_f = \frac{1}{\sqrt{3}}\, \sigma_f^E\, tg\theta, \tag{5.3}$$

where

$$\sigma_f^E = \sigma_\ell^* + \kappa\,(1 - e^{-n\varepsilon_f^E})\, \ln(Z_f^E/b), \tag{5.4}$$

ε_f^E is given by (4.7), and Z_f^E is the value at Σ_f of the Zener-Hollomon parameter.

It should be noticed that the jumps $\Delta\varepsilon_i$ and $\Delta\varepsilon_f$ do not lead to a variation of the structure but contribute to the adiabatic heating through ΔL_i and ΔL_f. Consequently, the terms in the left - hand side of the equivalence criteria (1.12) and (1.13) must be replaced for extrusion (E), respectively , by (4.7) and by

$$L_f^E = \int_0^{\varepsilon_f^E} \sigma(\varepsilon, Z^E)\, d\varepsilon. \qquad (5.5)$$

On the other hand, by (3.2), the evolution of the temperature field during extrusion can be determined by

$$T^E = T_i^E + \frac{1}{\rho c_v}(\Delta L_i + L^E), \qquad (5.6)$$

where T_i^E is the initial temperature of the billet at the begining of the deformation, and ΔL_i and L^E are given by (5.2) and (5.1). Finally, the temperature of the billet at the die exit is

$$T_f^E = T_i^E + \frac{1}{\rho c_v}(\Delta L_i + L_f^E + \Delta L_f), \qquad (5.7)$$

where L_f^E and ΔL_f are given by (5.5) and (5.3), respectively.

The next section will be devoted to the evalution of the initial temperature T_i^E.

6. ANALYSIS OF THE THERMAL FIELD BETWEEN WITHDRAWAL FROM FURNACE AND THE ENTRY TO THE DEFORMATION ZONE

A thorough experimental investigation of the evolution of thermal field during hot extrusion has been undertaken by HUGHES and SELLARS [16], who established a very precise balance between the heat loss of the billet to the atmosphere, the container, and the die on one side, and the heat gain resulting from the deformation on the other side. Billets for extrusion were machined from a previously wrought mild steel bar and were cut to give after upsetting a length of 2o.32 mm and a radius of R_i = 38.1 mm. The ram speeds used were v_i = 2.54 mm/s and 15.24 mm/s. The billet was heated to 117o°C and the container was

maintained at a constant temperature of 300°C. The total transfer time from the withdrawal from the furnace to the upsetting was 15 s, including about 7 s for rolling down the billet lubricant covered tray and about 8 s taken to set the pressing pad and for ram approach. Figs.2 and 3 show the temperature distribution $T(R, t)$ before entering the die, for R = const. and t = const., respectively [16].

Let Ω be the region inside the container and Σ_ℓ its cylindrical boundary. The evolution of the temperature field $T(R, t)$ in the billet before entering the die is governed by the differential equation with partial derivatives

$$\varrho c_v \frac{\partial T}{\partial t} + \operatorname{div} \underset{\sim}{q} = 0 \quad \text{in } \Omega, \tag{6.1}$$

the boundary condition

$$q_s \equiv \underset{\sim}{q} \cdot \underset{\sim}{n} = \eta (T_s - T^*) \quad \text{on } \Sigma_\ell, \tag{6.2}$$

and the initial condition

$$T(R,0) = T_0, \tag{6.3}$$

where $\underset{\sim}{q}$ is the heat flux vector, q_s is the heat flux across Σ_ℓ, $\underset{\sim}{n}$ is the outward unit normal to Σ_ℓ, η is a heat transfer coefficient across the film of lubricant, $T_s(t) = T(R_i, t)$, T^* is an effective temperature of the inner surface of the container and the lubricant, and T_0 is the temperature at the upsetting[x].

The heat flux vector is related to the temperature

---

x) We neglect in the following the slight radial inhomogeneity of the temperature field at upsetting, which may be produced by the free cooling of the billet during the transfer time.

gradient by Fourier's law

$$\underset{\sim}{q} = -\varkappa \, \mathrm{grad}\, T, \qquad (6.4)$$

where $\varkappa$ is the thermal conductivity of the billet. By introducing (6.4) into Eqs. (6.1) and (6.2), and taking into account that T depends only on R and t, we obtain

$$\rho c_v \frac{\partial T}{\partial t} - \frac{\varkappa}{R} \frac{\partial}{\partial R}\left(R \frac{\partial T}{\partial R}\right) = 0 \quad \text{in } \Omega, \qquad (6.5)$$

$$q_s \equiv -\varkappa \frac{\partial T}{\partial R} = \eta (T_s - T^*) \quad \text{on } \Sigma_\ell . \qquad (6.6)$$

Rigorously speaking, Eqs. (6.4) and (6.5) are valid only at sufficiently large distances from the die and the pad. However, as shown by HUGHES and SELLARS [16], the chilling produced by the heat loss to the die and to the pad do affect only the front and the back ends of the billet and have a minor influence on the central part of the billet.

In order to obtain the relation between the heat flux across Σ_ℓ and the evolution of the mean temperature on the cross section of the container

$$\overline{T}(t) = \frac{2}{R_i^2} \int_0^{R_i} R\, T(R,t)\, dR, \qquad (6.7)$$

we integrate Eq. (6.4) over the cross section and take into account $(6.5)_1$, thus obtaining

$$q_s = -\frac{\rho c_v R_i}{2} \frac{d\overline{T}}{dt} . \qquad (6.8)$$

By using the data in Fig.3 and numerically calculating the integral in (6.6) for t = const., HUGHES and SELLARS [16] obtained the evolution of $\overline{T}$ (t) and hence of $q_s(t)$. Next, correlating $q_s(t)$ with $T_s(t)$ they obtained the plot in Fig.4 which corresponds to the linear dependence (6.2) between q_s and T_s, and gives the numerical values η = 1.1 J/cm^2°C s and T^* = 510°C. The values of the material constants used in [16] have been ρ =7.86 g/cm^3.

c_v = 0.67 J/g°C at 1100°C, $\varkappa$ = 0.28 J/cm s°C at 1100°C. Finally, assuming that q_s and hence T_s do not depend on the billet radius R_i, HUGHES and SELLARS estimated the evolution of the mean temperature for billets of different diameters.

Since the assumption about T_s (t) being independent of R_i is essential for the determination of the temperature field in the billet we attempted to verify the validity of this hypothesis by using the exact solution of Eq. (6.5) satisfying the boundary condition (6.6) and the initial condition (6.3) which reads (see, e.g., TOLSTOV [17]):

$$T(R,t) = T^* + \sum_{n=1}^{\infty} A_n J_0(\lambda_n R)\, e^{-k^2\lambda_n^2 t}\,, \qquad (6.9)$$

where

$$\lambda_n = \frac{\mu_n}{R_i}\,, \qquad k^2 = \frac{\varkappa}{\varrho c_v}\,, \qquad (6.10)$$

$$A_n = \frac{2(T_0 - T^*)\, J_1(\mu_n)}{\mu_n \left[J_0'^2(\mu_n) + J_0^2(\mu_n) \right]}\,, \qquad (6.11)$$

J_0 and J_1 are Bessel functions of zeroth and first order, respectively , and μ_n, n = 1,2,...., are the roots of the equation

$$\mu J_0'(\mu) + A J_0(\mu)\,, \qquad A = \eta R_i/\varkappa\,. \qquad (6.12)$$

Taking into account that $J_0'(R) = -J_1(R)$, we obtain from $(6.12)_1$

$$J_0'(\mu_n) = -J_1(\mu_n) = \frac{A}{\mu_n} J_0(\mu_n),$$

and hence (6.11) becomes

$$A_n = \frac{2(T_0 - T^*)\, A}{(A^2 + \mu_n^2)\, J_0(\mu_n)}\,. \qquad (6.13)$$

By substituting this result into (6.9) and setting $R = R_i$, we obtain the surface temperature

$$T_s(t) = T^* + (T_0 - T^*) \sum_{n=1}^{\infty} \frac{2A}{A^2 + \mu_n^2}\, e^{-k^2\lambda_n^2 t}\,. \qquad (6.14)$$

For sufficiently small values of t the exponentials in (6.14) may be approximated as

$$e^{-k^2\lambda_n t} \simeq \frac{1}{1+k^2\lambda_n^2 t} = \frac{C^2}{C^2+\mu_n^2},$$

where $C = C(t) = R_i/(k\sqrt{t})$. Hence (6.14) may be rewritten in the approximate form

$$T_s(t) = T^* + \frac{T_o - T^*}{C^2 - A^2}\left(C^2 \sum_{n=1}^{\infty} \frac{2A}{A^2+\mu_n^2} - AC \sum_{n=1}^{\infty} \frac{2C}{C^2+\mu_n^2}\right). \qquad (6.15)$$

On the other hand, we have the identity [17]

$$\sum_{n=1}^{\infty} \frac{2A}{A^2+\mu_n^2} = 1 \qquad (6.16)$$

for any positive A provided that μ_n are the roots of Eq.(6.12). Moreover, since the roots of Eq.(6.12) are approximately independent of A for large values of A, a condition that is always satisfied within our field of interest, we may admit that the identity (6.16) is still fulfilled when replacing A by C(t), for small values of t. Consequently, Eq.(6.15) becomes

$$T_s(t) = T^* + \frac{(T_o - T^*)C}{C+A} = T^* + \frac{T_o - T^*}{1+(\eta k/\varkappa)\sqrt{t}}. \qquad (6.17)$$

This relation shows that the surface temperature of the billet before entering the die is indeed independent of R_i within the range of validity of our approximations.

Since the exact solution is expressed in (6.9) by a slowly convergent series, we attempted to derive also an approximate but simpler form of the temperature field.

Analyzing data in Fig.2 and 3 leads to the conclusion that the isotherms T(R, t) = const. are straight lines in the plane (R, t). Hence we may write

$$t = t_a(T) + [t_s(T) - t_a(T)](R/R_i), \qquad (6.18)$$

where $t_a(T)$ and $t_s(T)$ are the times at which the temperature

takes the value T in the axis of the billet, respectively on its surface. (Fig.5). We shall use in the following Eq. (6.18) in order derive the evolution of the temperature in the axis of the billet $T_a(t) = T(0, t)$.

By differentiating Eq.(6.18) with respect to R and putting $R = R_i$ we deduce

$$R_i\, t'_s(T_s) \left.\frac{\partial T}{\partial R}\right|_{R=R_i} + t_s(T_s) - t_a(T_s) = 0. \qquad (6.19)$$

Inspection of Fig.2 reveals that $t_s(T_s) \ll t_a(T_s)$ for $T_s > T_o$, such that $t_s(T_s)$ may be neglected in (6.19). Considering also the boundary condition (6.6), it results from (6.19) that

$$t_a(T_s) = -(R_i \eta/\varkappa)\, t'_s(T_s)\,(T_s - T^*).$$

Since this relation is valid for any $T_s \in (T_o, T^*)$ we may also write

$$t_a(T) = -(R_i \eta/\varkappa)\, t'_s(T)\,(T - T^*). \qquad (6.20)$$

On the other hand, Fig.2 shows that $t_a(T)$ is approximately a linear function of $T - T_o$ at least for the small time elapse between upsetting and the beginning of deformation. Therefore, we can write

$$t_a(T) = k_a\,(T - T_o), \qquad (6.21)$$

where, by (6.20),

$$k_a = \lim_{T \to T_o} t'_a(T) = -(R_i \eta/\varkappa)\left[t''_s(T_o)(T_o - T^*) + t'_s(T_o)\right]. \qquad (6.22)$$

In order to calculate the values of $t'_s(T_o)$ and $t''_s(T_o)$ we solve (6.17) with respect to t, thus obtaining for small positive values of $T - T_o$

$$t_s(T) = \frac{\varkappa \varrho c_v}{\eta^2}\left(\frac{T_o - T}{T - T^*}\right)^2,$$

wherefrom it follows that

$$t'_s(T_o) = 0, \qquad t''_s(T_o) = \frac{2\varkappa \varrho c_v}{\eta^2}\,\frac{1}{(T_o - T^*)^2}.$$

Introducing these expressions into (6.22) and (6.21) it results

$$t_a(T) = -\frac{2R_i \rho c_v}{\eta(T_o - T^*)} (T - T_o). \qquad (6.23)$$

Finally, by solving this equation for T gives

$$T_a(t) = T_o - \frac{\eta(T_o - T^*)}{2R_i \rho c_v} t. \qquad (6.24)$$

It is to be expected that the ratio $\eta(T_o - T^*)/(\rho c_v)$ does not vary strongly for different steel grades and hot extrusion processes. Consequently, the prefactor of t in (6.24) is mainly influenced by the radius R_i of the billet. Thus, denoting by $T_a^{HS}(t)$ the axial temperature measured by HUGHES and SELLARS [16] and by R_i^{HS} the radius of the billet used in their experiment (38.1 mm), we deduce from (6.24) that

$$\frac{T_a(t) - T_o}{T_a^{HS}(t) - T_o^{HS}} = \frac{R_i^{HS}}{R_i},$$

and hence

$$T_a(t) = T_o - (R_i^{HS}/R_i)\left[T_o^{HS} - T_a^{HS}(t)\right]. \qquad (6.25)$$

This simplified equation will be used in the following for simulating the hot extrusion together with the relation

$$T_s(t) = T_s^{HS}(t) \qquad (6.26)$$

which results from (6.17) when neglecting the variation of the parameter $(T_o - T^*)\eta/\sqrt{\rho \varkappa c_v}$ for different steel grades and extrusion processes.

It should be noticed, however, that Eqs. (6.24) and (6.17) allow the evaluation of $T_a(t)$ and $T_s(t)$ even for other values of the parameters ρ, c_v, $\varkappa$, η, and $T_o - T^*$.

7. THERMOMECHANICAL SIMULATION OF THE DEFORMATION DURING THE HOT EXTRUSION

In this section we shall use the equivalence criteria formulated in Sect.1 as well as the results obtained in Sects. 4 - 6 concerning the evolution of the thermokinematic fields during hot extrusion in order to design the simulating torsion tests.

The furnace and container temperatures and the transfer time are chosen as in the experiment of HUGHES and SELLARS [16]. However, we take the radius of the billet $R_i = 75$ mm, the length of the billet $L = 600$ mm, the semicone die angle $\alpha = 70^\circ,3$, and the ram speed $v_i = 150$ mm/s. By using AVITZUR's analysis [15], Chap.8) and taking the Coulomb coefficient of friction between the metal and the die $\mu = 0.08$, it may be shown that there exists no dead zone, and hence the semicone angle α_1 of the deformation zone should be taken in our case equal to α (see also Fig.1).

Since the thermokinematic fields in the billet are highly inhomogeneous it is necessary to use several torsion tests in order to simulate the deformation of different zones of the billet. Therefore, we choose four typical points of the billet, whose positions at the upsetting are labeled by 1, 2, 3, 4 in Fig.6.

As the temperature at the withdrawal from furnace ($T_o = 1170^\circ C = 1443$ K) and the transfer time $t_t = 15$ s have been chosen equal to those in [16], we may extend the applicability of Eqs. (6.25) and (6.26) to the whole time elapse from the withdrawal from furnace to the die entry.

Therefore, the temperatures T_i^E at the die entry are calculated by the formulae

$T_i^E = T_a(t_t)$ for point 1 , $T_i^E = T_s(t_t)$ for point 2 ,

$T_i^E = T_a(t_t+L/v_i)$ for point 3, $T_i^E = T_s(t_t+L/v_i)$ for point 4,

where t_t=15 s is the transfer time, and $T_a(t)$, $T_s(t)$ are calculated by (6.25) and (6.26), respectively, with T_o = 1170°C = 1433 K (the temperature at the withdrawal from furnace), t being the time measured after withdrawal from furnace. The values of T_i^E calculated in this way are given in the third column of Table 1.

For the sake of convenience we recollet here the basic formulae characterising the evolution of thermokinematic fields during hot extrusion (cf. Sects. 2- 5).

The strain rate intensity is

$$\dot{\varepsilon}^E = \dot{\varepsilon}_i^E \exp \frac{3\,\varepsilon^E \cos\theta}{2\sqrt{1-\frac{11}{12}\sin^2\theta}}, \tag{7.1}$$

where

$$\dot{\varepsilon}_i^E = \frac{2v_i}{r_i}\sqrt{1-\frac{11}{12}\sin^2\theta} \tag{7.2}$$

is the initial value of $\dot{\varepsilon}^E$, and ε^E is the strain intensity varying from 0 to its final value

$$\varepsilon_f^E = \frac{2\sqrt{1-\frac{11}{12}\sin^2\theta}}{\cos\theta}\ln\frac{R_i}{R_f}. \tag{7.3}$$

The work done per unit volume up to a current strain intensity ε^E is

$$L^E = \int_0^{\varepsilon^E} \sigma(\varepsilon, Z^E)\,d\varepsilon, \tag{7.4}$$

where the stress intensity σ is given by the constitutive equation

$$\sigma(\varepsilon,Z) = \begin{cases} [a + c(1-e^{-n\varepsilon})]\ln(Z/b) & \text{if } Z \le Z_\ell \\ \sigma_\ell^* + c(1-e^{-n\varepsilon})\ln(Z/b) & \text{if } Z > Z_\ell . \end{cases} \tag{7.5}$$

The current value of the Zener-Hollomon parameter is

$$Z^E = \dot{\varepsilon}^E \exp\frac{Q}{RT^E}, \tag{7.6}$$

and the values of the material constants a, b, c, n, Q, Z_ℓ, σ_ℓ^* for the AISI 316L stainless steel are (2.8) and (2.9). The evolution of the temperature field is given by

$$T^E = \tilde{T}_i^E + \frac{L^E}{\rho c_v}, \tag{7.7}$$

where

$$\tilde{T}_i^E = T_i^E + \frac{\sigma_\ell^* \operatorname{tg}\theta}{\sqrt{3}\,\rho c_v} \tag{7.8}$$

is the value of temperature of the particles after traversing the discontinuity surface Σ_i.

The numerical integration of the above system of equations is done by a step - by - step method, using the following iteration scheme with M steps:

$$\varepsilon_k^E = k\varepsilon_1, \quad \varepsilon_1 = \varepsilon_f^E/M, \quad k = 0,1,\dots,M,$$

$$\dot{\varepsilon}_k^E = \dot{\varepsilon}_i^E \exp \frac{3\,\varepsilon_k^E \cos\theta}{2\sqrt{1-\frac{11}{12}\sin^2\theta}},$$

$$L_k^E = L_{k-1}^E + \sigma_{k-1}^E \varepsilon_1,$$

$$T_k^E = \tilde{T}_i^E + \frac{L_k^E}{\rho c_v},$$

$$Z_k^E = \dot{\varepsilon}_k^E \exp \frac{Q}{RT_k^E},$$

$$\sigma_k^E = \begin{cases} [a + c(1-e^{-n\varepsilon_k^E})] \ln(Z_k^E/b) & \text{if } Z_k^E \le Z_\ell \\ \sigma_\ell^* + c(1-e^{-n\varepsilon_k^E}) \ln(Z_k^E/b) & \text{if } Z_k^E > Z_\ell. \end{cases}$$

The initial values of the iteration variables are

$$\varepsilon_o^E = 0, \quad \dot{\varepsilon}_o^E = \dot{\varepsilon}_i^E, \quad L_o^E = 0, \quad T_o^E = \tilde{T}_i^E,$$

$$Z_o^E = \dot{\varepsilon}_o^E \exp(Q/R\tilde{T}_i^E),$$

$$\sigma_o^E = \begin{cases} a \ln (Z_o^E / b) & \text{if } Z_o^E \leq Z_\ell \\ \sigma_\ell^* & \text{if } Z_o^E > Z_\ell . \end{cases}$$

The calculation was performed on a TI 58 minicomputer, by using a specially constructed program called EXTRUD, taking M = 40 and M = 200 steps; the difference between the final values of the integration variables in the two variants were less than 4%.

The initial and final values of the integration variables are given in Table 1, and the plots of $\dot{\varepsilon}^E, \sigma^E, L^E, T^E$, and Z^E against $\varepsilon^E / \varepsilon_\ell^E$ are shown in Figs. 7-11. It may be seen that the variables associated with the particles 1, 2 , and 3 have similar evolutions, whereas the particle 4, which has the smallest die entry temperature, experiences a stress intensity and a temperature increase during the deformation that are about 2.5 times greater than those corresponding to the other three particles.

For specimens used in our torsion tests, the surface strain intensity ε_s^T and strain rate intensity $\dot{\varepsilon}_s^T$ are given by

$$\varepsilon_s^T = \frac{2\pi r_o n}{\ell \sqrt{3}} \simeq 0.218\, n, \qquad \dot{\varepsilon}_s^T\,[s^{-1}] = \frac{2\pi r_o N}{60 \ell \sqrt{3}} \simeq 0.00363\, N\,[\text{rev/min}], \tag{7.9}$$

where ℓ = 50 mm and r_o = 3 mm are the length and the radius of the specimens, respectively, n is the number of revolutions, and N is the torsion speed.

By using the first equivalence criterion (1.12), we obtain the number of revolutions

$$n_f = \frac{\varepsilon_f^E}{0.218}, \tag{7.10}$$

for which the final value of the torsion surface strain intensity ε_{sf}^T equals the final value of the extrusion strain intensity for the

particle under consideration.

Next, by substituting (2.12) into the second equivalence criterion (1.13) and taking into account that $\varepsilon_{sf}^T = \varepsilon_f^E$, we obtain

$$k_L = \frac{L_f^E}{\varepsilon_f^E}$$

or, by (2.13),

$$a_L \left(\ln \dot{\varepsilon}_s^T + \frac{Q_L}{R T_i^T} - \ln b_L \right) = \frac{L_f^E}{\varepsilon_f^E} . \qquad (7.11)$$

This relation allows determining either the torsion speed N or the initial torsion temperature T_i^T, when the other quantity is prescribed, by using one of the formulae

$$N = 0.00363\, b_L \exp\left(\frac{L_f^E}{a_L \varepsilon_f^E} - \frac{Q_L}{R T_i^T} \right), \qquad (7.12)$$

$$T_i^T = \frac{Q_L / R}{L_f^E / (a_L \varepsilon_f^E) - \ln (\dot{\varepsilon}_s^T / b_L)} . \qquad (7.13)$$

Eqs. (7.1o), (7.12), and (7.13) give the parameters of the simulating torsion test. For illustration they have been applied for the typical particles 1, 2, 3, 4 in the hot extrusion of the AISI 316L stainless steel, choosing N = 1500 rev/min. The values resulted for n_f and T_i^T are given in the last two columns of Table 1.

8. CONCLUSIONS

The theoretical analysis of the hot working processes shows that hot torsion tests provide a reliable means for simulating these processes. This simulation is based on two equivalence criteria, namely the equality of the final strain intensities and of the plastic work done per unit volume during the deformation in the technological process and the torsion test. The application of

the simulation procedure requires the knowledge of the constitutive equations of the investigated materials for the whole strain, strain rate, and temperature ranges of the working process and the simulating test.

Various simplifying hypotheses that relax those adopted in [1, 2] but still facilitate the practical application of the simulation have been analyzed. Finally , the simulation procedure has been applied for the hot extrusion of the AISI 316L austenitic stainless steel, the parameters of the simulating torsion test being calculated for four different characteristic points of the billet. The evolution of the thermokinematic fields during extrusion have been calculated by adopting an admissible kinematic field and using the experimental results of HUGHES and SELLARS [16] for hot extrusion. A more exact evaluation of these fields requires the solving of the non-linear initial and boundary-value problems involved, by using the finit elements methods.

Table 1

Particle	Θ [deg]	T_i^E [K]	$\tilde{T}_i^E$ [K]	$\dot{\varepsilon}_i^E$ [s^{-1}]	ε_f^E	$\dot{\varepsilon}_f^E$ [s^{-1}]	L_f^E [MPa]	T_f^E [K]	n_f [rev]	T_i^T [K]
1	0	1437	1437	3.76	2.75	231.98	434	1519	12.61	1362
2	7o.3	1363	1399	1.63	3.53	1oo.43	557	15o5	16.19	1362
3	0	142o	142o	3.76	2.75	231.98	457	15o7	12.61	1342
4	7o.3	917	1oo7	1.63	3.53	1oo.43	1144	1224	16.19	1o87

FIGURE CAPTIONS

Fig:1. Admissible velocity field for extrusion.

Fig.2 Cooling curves at different depths (R = const.), from the billet surface (after HUGHES and SELLARS [16]).

Fig.3 Radial variation of the temperature in the billet at different times after upsetting in the container (after HUGHES and SELLARS [16]).

Fig.4. Correlation of the heat flux across the cylindrical surface of the billet with the surface temperature of the billet (after HUGHES and SELLARS [16]).

Fig. 5 Isotherms of the temperature field in the billet after upsetting.

Fig.6. Billet, container, and die geometry; ① - ④: characteristic particles of the billet.

Fig.7. Evolution of the strain rate intensity during hot extrusion.

Fig.8. Evolution of the stress intensity during hot extrusion.

Fig.9. Evolution of the plastic work done per unit volume during hot extrusion.

Fig.1o. Evolution of the thermal field during hot extrusion.

Fig.11. Evolution of the Zener-Hollomon parameter during hot extrusion.

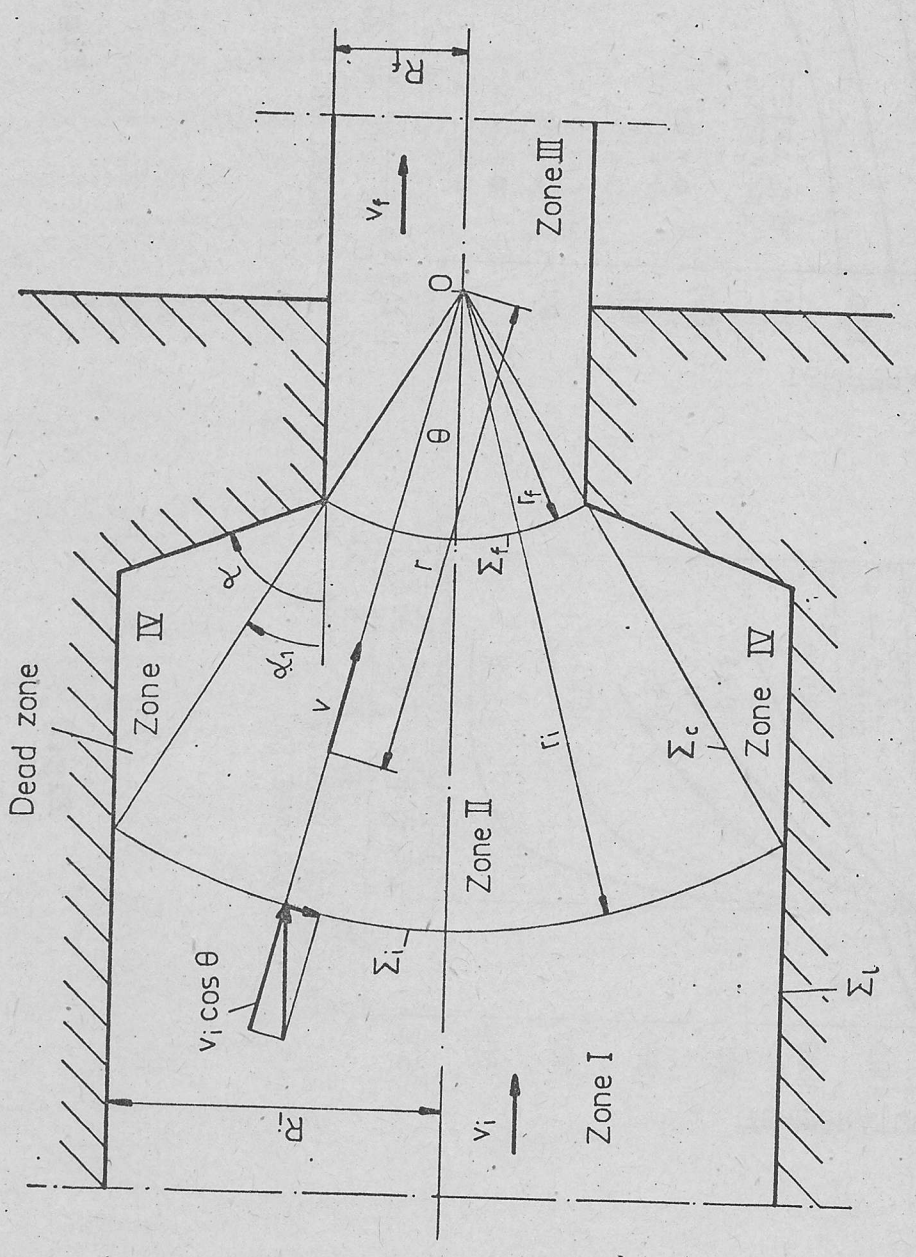
Dead zone
Zone IV
Zone II
Zone I
Zone III
Zone IV
R_f
v_f
O
θ
r_f
Σ_f
α
α_1
r
v
r_i
Σ_c
Σ_i
$v_i \cos\theta$
R
v_i
Σ_l

Fig.1

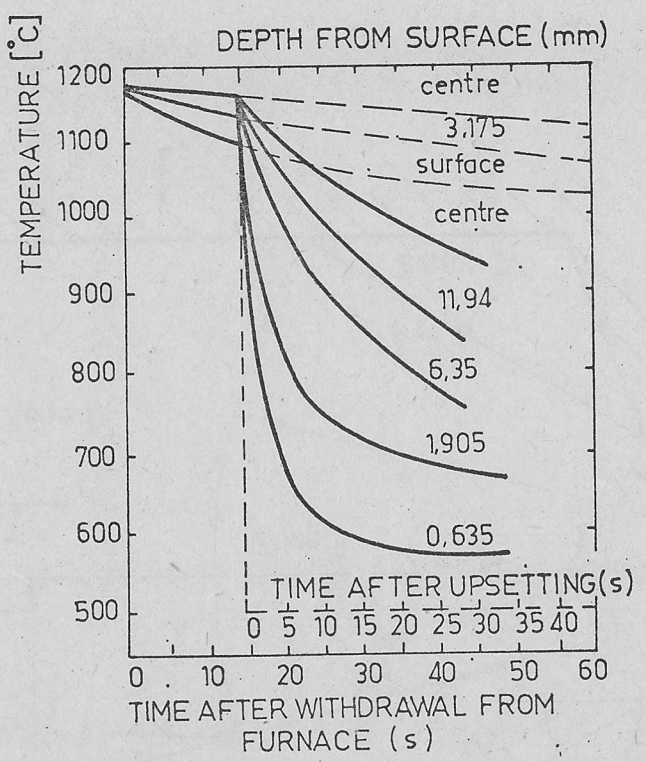
DEPTH FROM SURFACE (mm)
TEMPERATURE [°C]
1200
1100
1000
900
800
700
600
500
centre
3,175
surface
centre
11,94
6,35
1,905
0,635
TIME AFTER UPSETTING(s)
0 5 10 15 20 25 30 35 40
0 10 20 30 40 50 60
TIME AFTER WITHDRAWAL FROM FURNACE (s)

Fig.2

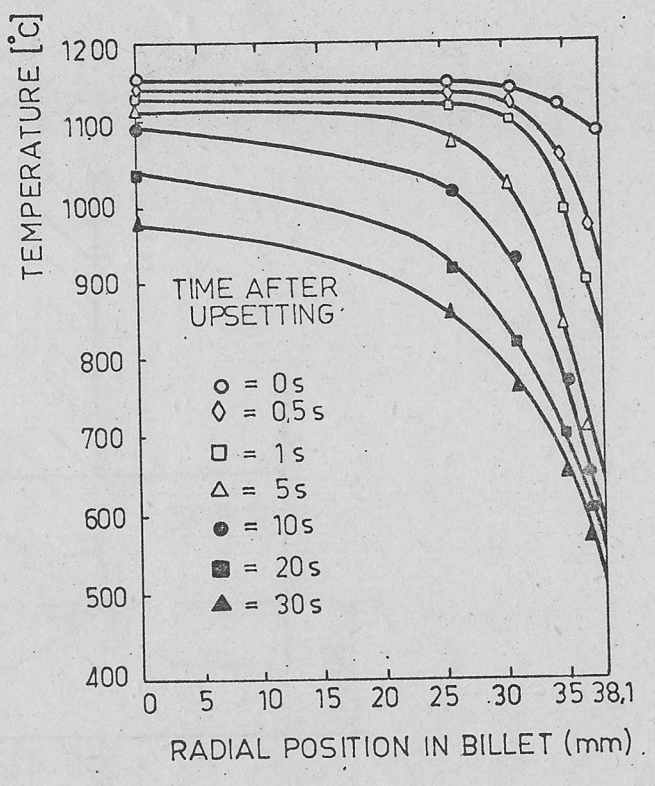
TEMPERATURE [°C]
1200
1100
1000
900
800
700
600
500
400
TIME AFTER UPSETTING
o = 0s
◇ = 0,5s
□ = 1s
△ = 5s
● = 10s
■ = 20s
▲ = 30s
0 5 10 15 20 25 30 35 38,1
RADIAL POSITION IN BILLET (mm)

Fig.3

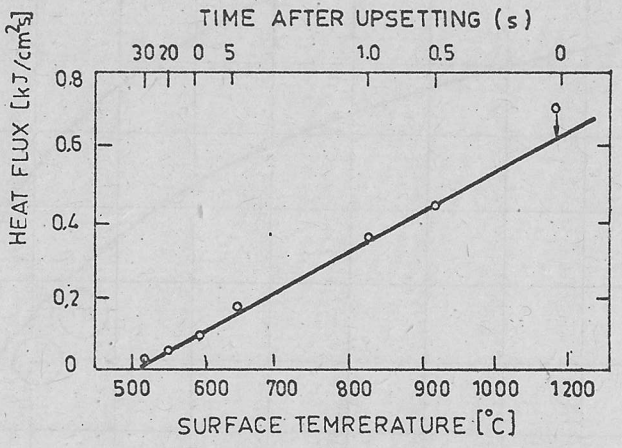
TIME AFTER UPSETTING (s)
30 20 0 5 1.0 0.5 0
HEAT FLUX [kJ/cm²s]
0.8
0.6
0.4
0.2
0
500 600 700 800 900 1000 1200
SURFACE TEMRERATURE [°C]

Fig.4

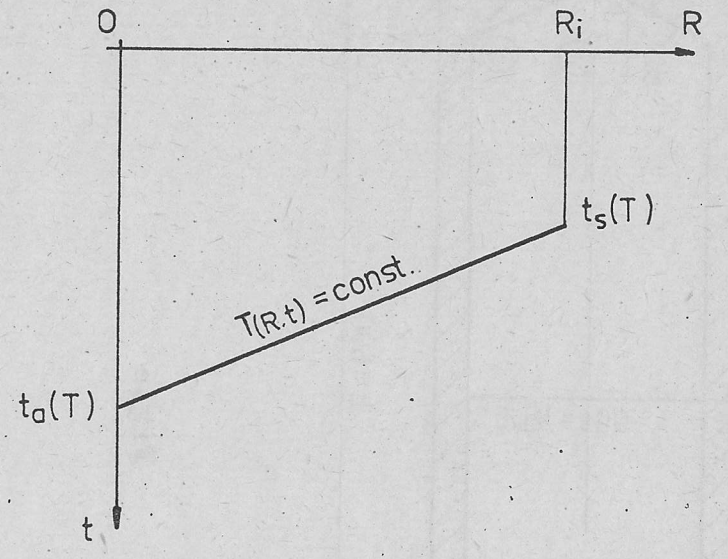
O
Rᵢ
R
tₛ(T)
T(R.t) = const.
tₐ(T)
t

Fig.5

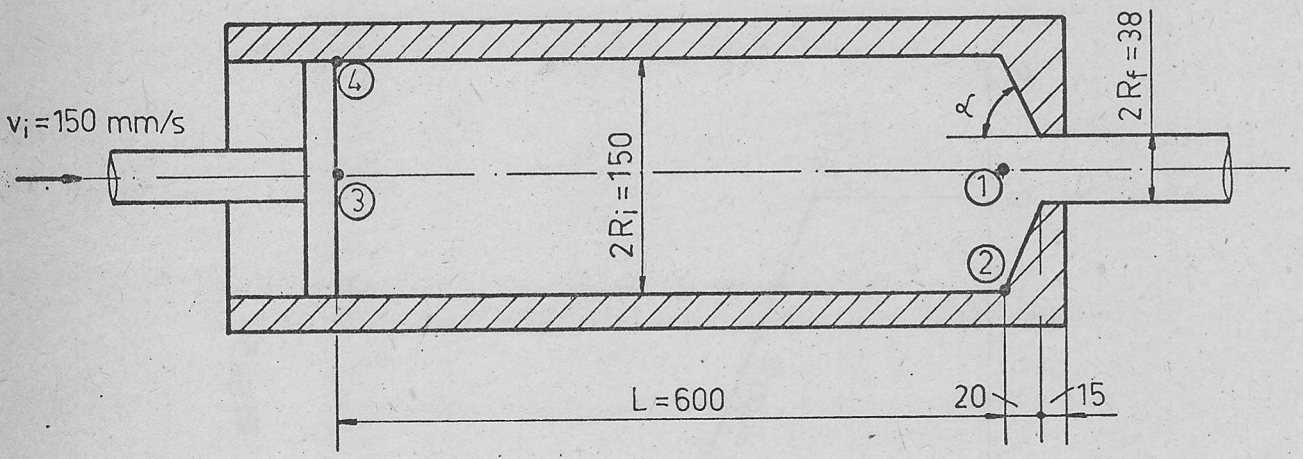
v_i = 150 mm/s
4
3
$2R_i$ = 150
α
$2R_f$ = 38
1
2
L = 600
20
15

Fig.6

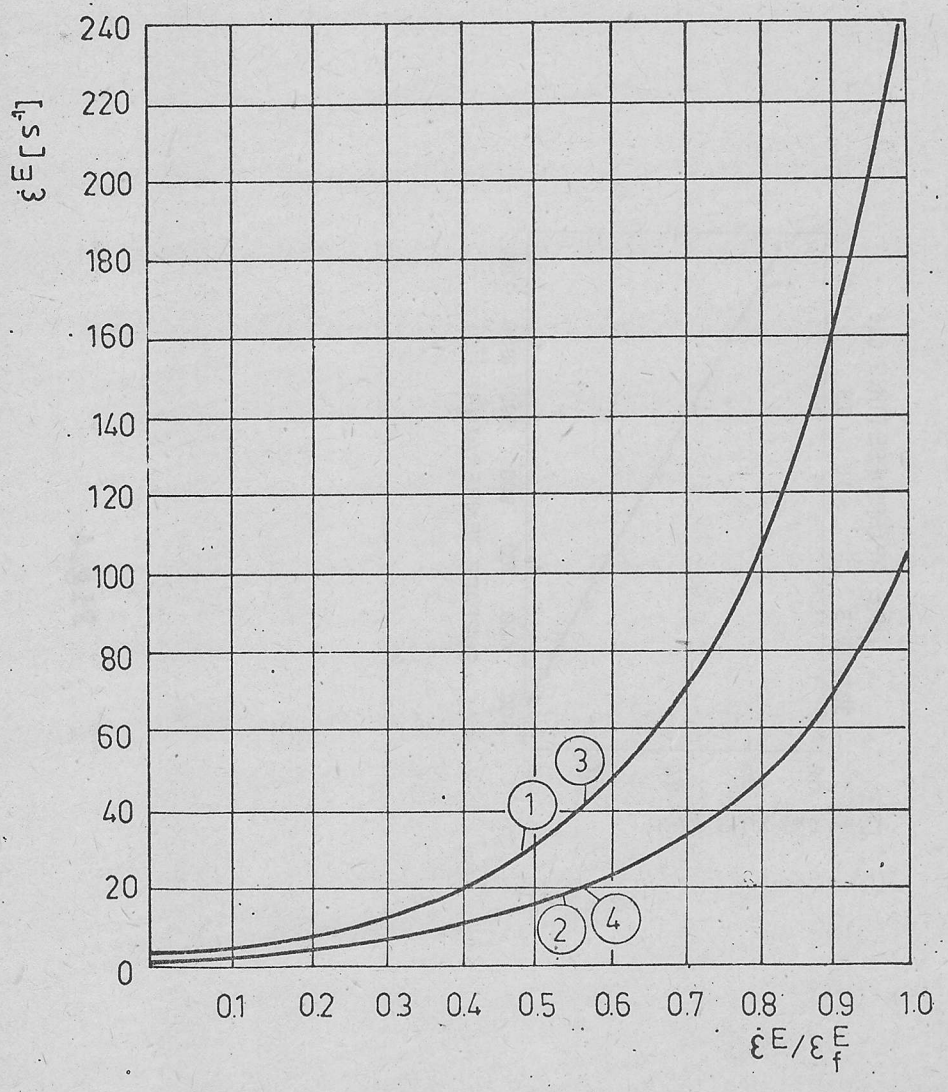
$\dot{\varepsilon}^E$ [s^{-1}]
240
220
200
180
160
140
120
100
80
60
40
20
0
0.1
0.2
0.3
0.4
0.5
0.6
0.7
0.8
0.9
1.0
$\dot{\varepsilon}^E/\dot{\varepsilon}^E_f$
1
2
3
4

Fig.7

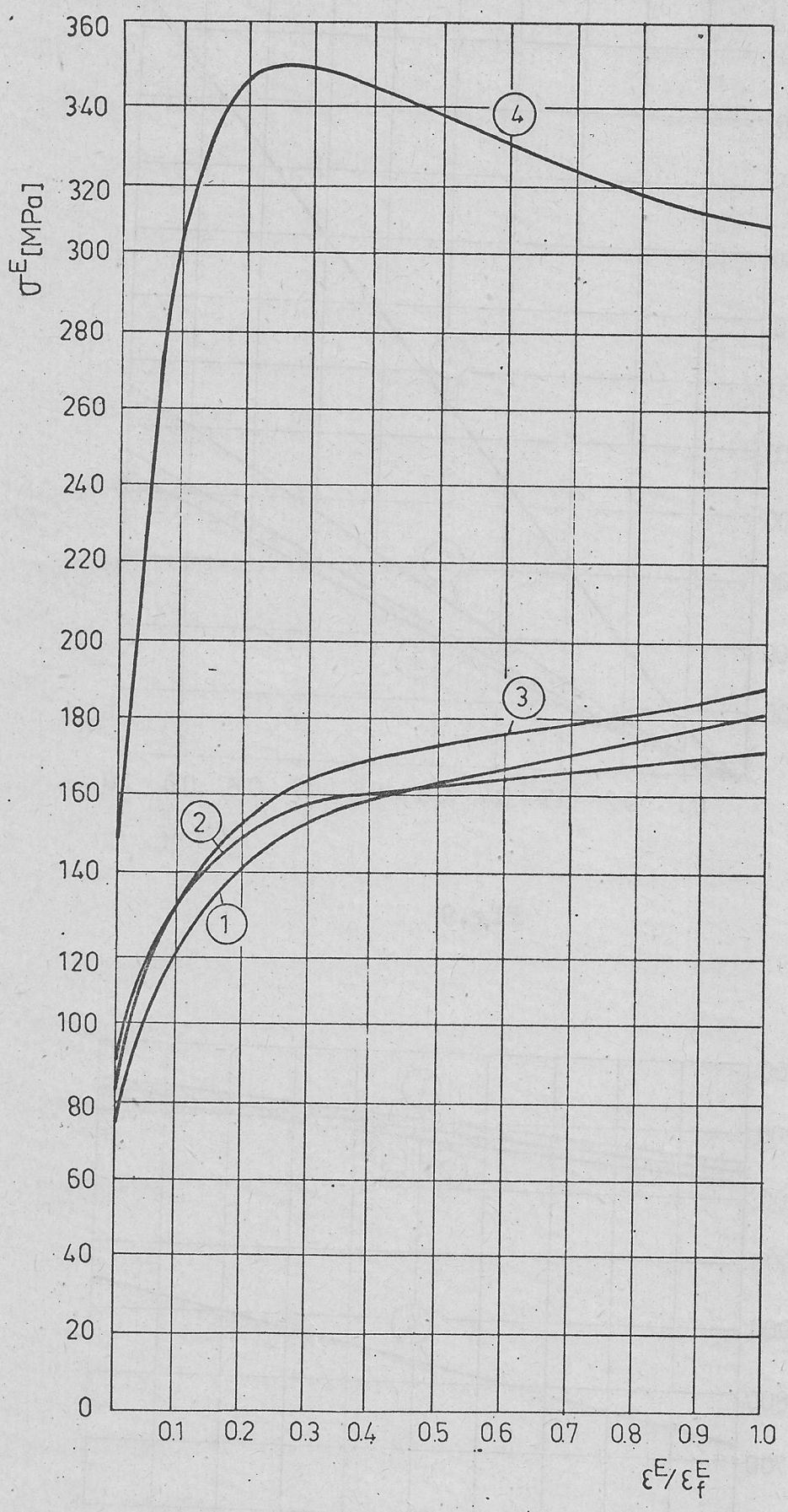
360
340
320
300
280
260
240
220
200
180
160
140
120
100
80
60
40
20
0
σ^E[MPa]
0.1
0.2
0.3
0.4
0.5
0.6
0.7
0.8
0.9
1.0
$\varepsilon^E/\varepsilon_f^E$
1
2
3
4

Fig.8

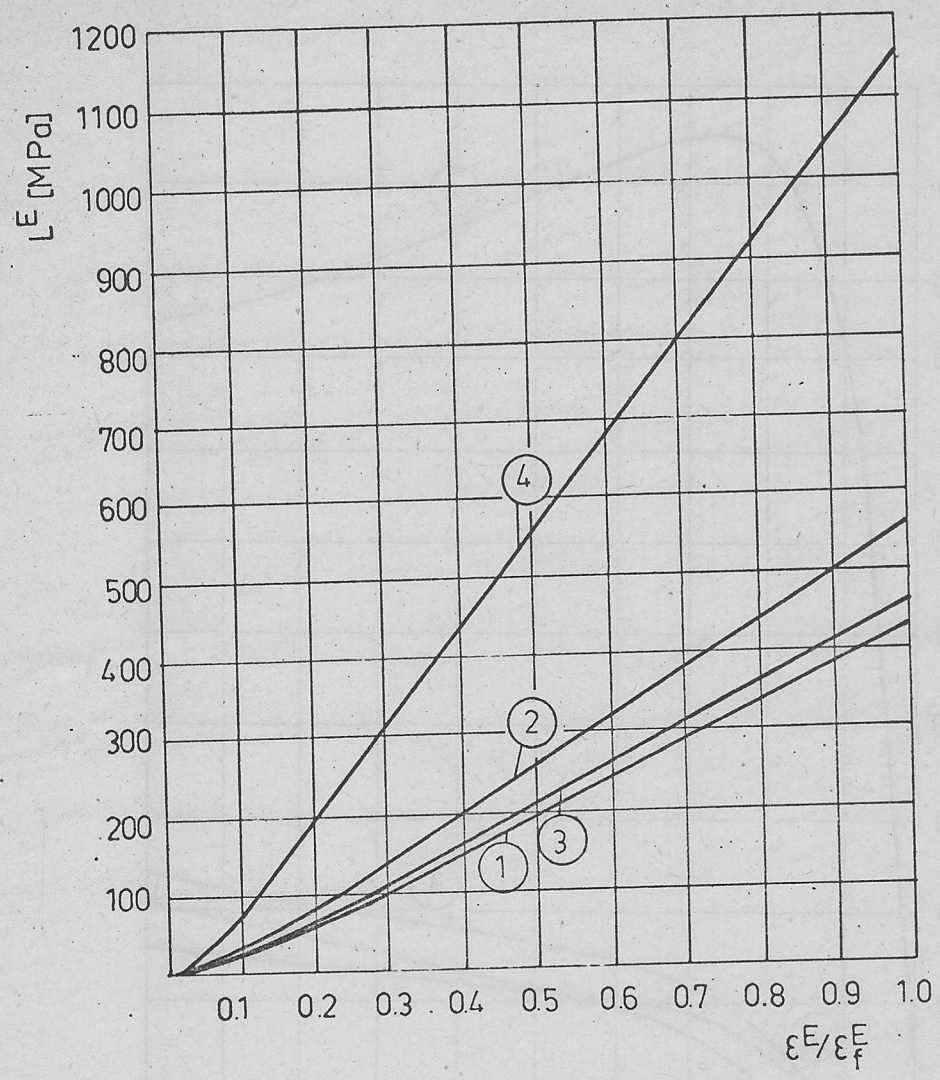
L^E [MPa]
1200
1100
1000
900
800
700
600
500
400
300
200
100
0.1
0.2
0.3
0.4
0.5
0.6
0.7
0.8
0.9
1.0
$\varepsilon^E/\varepsilon_f^E$
1
2
3
4

Fig.9

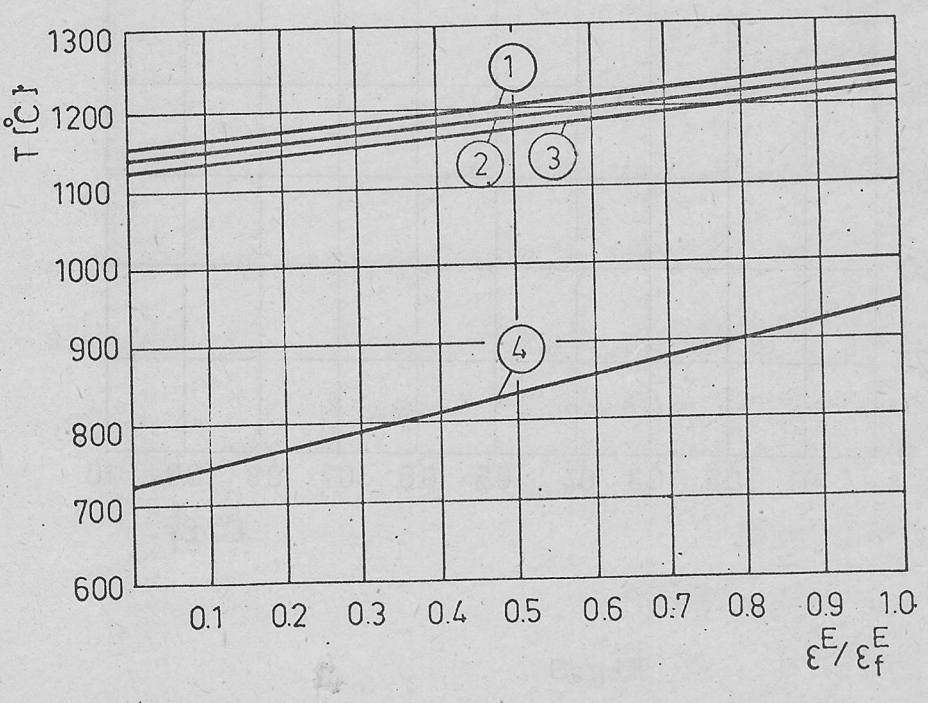
T [°C]
1300
1200
1100
1000
900
800
700
600
0.1
0.2
0.3
0.4
0.5
0.6
0.7
0.8
0.9
1.0
$\varepsilon^E/\varepsilon_f^E$
1
2
3
4

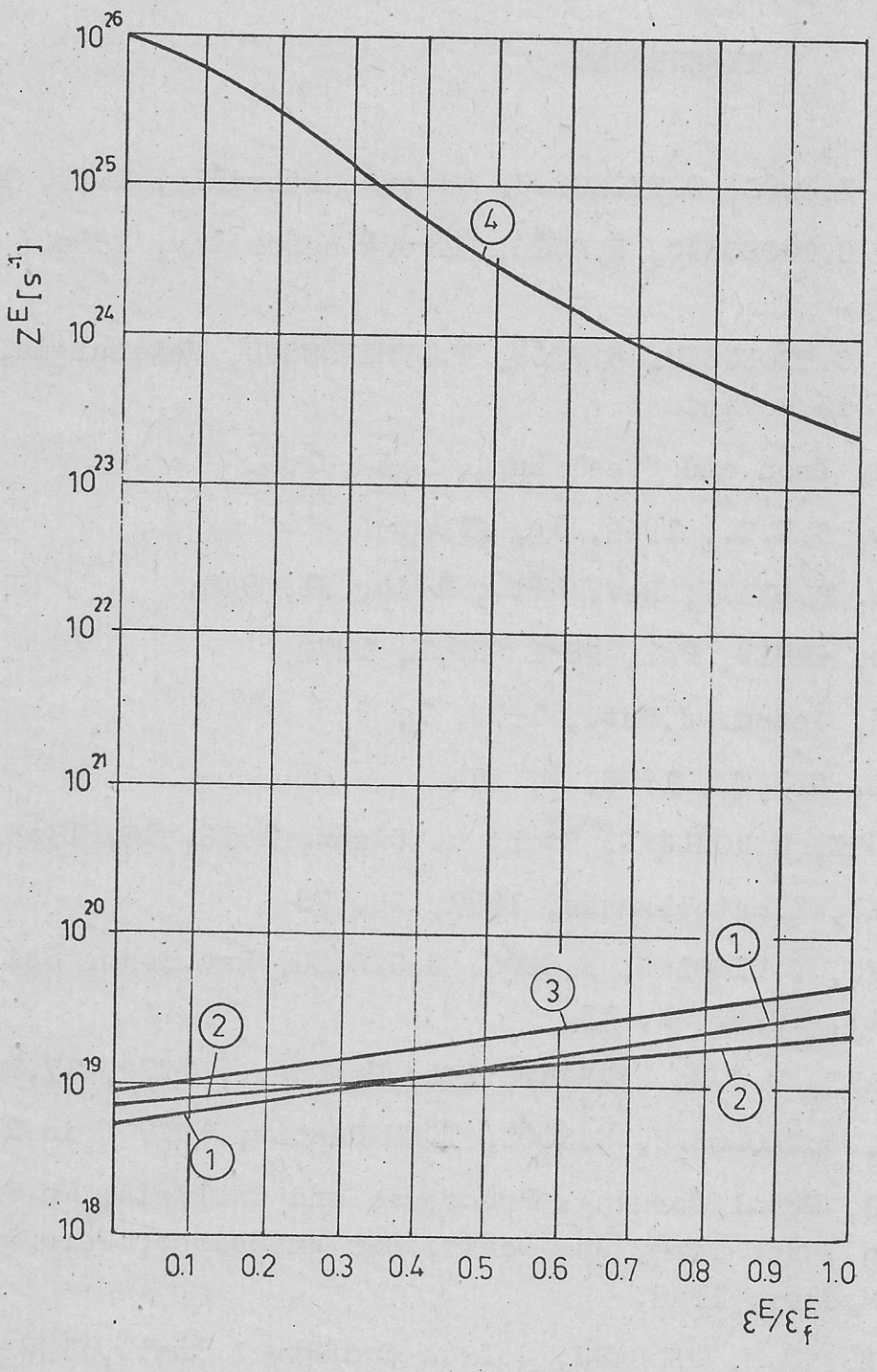
10^{26}
10^{25}
10^{24}
10^{23}
10^{22}
10^{21}
10^{20}
10^{19}
10^{18}
$Z^E [s^{-1}]$
0.1
0.2
0.3
0.4
0.5
0.6
0.7
0.8
0.9
1.0
$\varepsilon^E/\varepsilon_f^E$
1
2
3
4

Fig.11

REFERENCES

1. C.G.RADU, E.SOÓS, C.TEODOSIU, Kovové materiály, 1979, 17,433.
2. C.G.RADU, C.TEODOSIU, E.SOÓS, Kovové materiály, 1980 (to be published).
3. C.G.RADU, C.TEODOSIU, E.SOÓS, T.DUMITRESCU, Metalurgia, 1979, 31, 580 (in Romanian)
4. B.AVITZUR, Iron and Steel Eng., 1962, 1o4.
5. C.ROSSARD, C.I.T., 1962, 1o, 2199.
6. C.ROSSARD, P.BLAIN, Rev. Mét., 1964, 61, 949.
7. C.ROSSARD, IRSID, PA1, 2831 CRIBH, 1972.
8. K.NIKKILÄ, Scand. J.Met., 1972, 1, 9
9. A.FAESSEL, C.I.T., 1976, 4, 874.
1o. E.NEUSCHÜTZ, H.ROHLOFF, Stahl u. Eisen, 1976, 96, 13o3.
11. O.PAWELSKI, Z.Metallkunde, 1977, 68, 79
12. C.TEODOSIU, V.NICOLAE, E.SOÓS, C.G.RADU, Rev.Roum. Sci. Tehn.-Méc. Appl., 1979, 24, 13.
13. C.M.SELLARS, W.J.Mc. TEGART, Int. Met.Rev., 1972, 17,1.
14. C.G.RADU, C.TEODOSIU, E.SOÓS, ICEM Report, 1979 (in Romanian)
15. B.AVITZUR, Metal forming: Processes and analysis, Mc Graw - Hill Book Comp., New York, St. Louis, San Francisco, Toronto, London, Sydney, 1968.
16. K.E.HUGHES, C.M. SELLARS, J.Iron and Steel Inst., 1972, 21o, 661
17. G.P.TOLSTOV , Fourier Series, 2 nd Ed., Fizmatghiz, Moscow, 196o (in Russian)